

6. BACKGROUND ESTIMATION METHODS

Having completed our description of the various SM and non-collision backgrounds, we now turn our attention to predicting the number of events we expect from each in the signal region for our final sample. This process is purely based on data-driven methods and is a multi-step process. We will address each step in turn.

Since the two dominant backgrounds are wrong vertex SM events with an unknown mean and cosmic ray events we describe their rates one at a time. Section 6.1 provides an overview of how we will use the double Gaussian nature of the timing distributions in order to perform a data-driven background estimation of the wrong vertex mean. Furthermore we demonstrate that if we know the mean of the wrong vertex distribution we are able to predict the number of events expected in the signal region from SM sources from data-only methods.

Since an important piece of the SM estimate is the determination of the wrong vertex mean, in Section 6.2 we detail a data-driven method to obtain a good estimate of the wrong vertex mean. This is done using a second sample of events that has identical cuts to the signal region, but with one requirement reversed. This allows the sample to be independent but have similar properties that should allow us to measure the mean of the wrong vertex distribution. In particular, we select a sample of events passing all the exclusive $\gamma + \cancel{E}_T$ events (found in Table 5.5) but failing to reconstruct a vertex. We call this sample the “no vertex sample”.

This sample is particularly useful because, as we will show, the mean of the t_{corr}^0 distribution, $\langle t_{corr}^0 \rangle$, should reproduce the mean of wrong vertex sample, $\langle t_{corr}^{WV} \rangle$, within small uncertainties. Then, using our six MC control samples and two $e + \cancel{E}_T$ control samples we will show that $\langle t_{corr}^0 \rangle = \langle t_{corr}^{WV} \rangle$ to within 80 ps. This value will serve as a systematic uncertainty which will be taken into account in the final estimation of the number of events in the signal region. Finally, in Section 6.3 we will lay out the final procedure for predicting the expected number of events in the

signal region from SM sources along with the contribution from cosmic rays for a final predicted value.

6.1 Overview of Data-Driven Background Method for Collision Backgrounds

We can use the data and an understanding of the shape of the wrong vertex timing distribution to predict the number of events in the signal region from collision backgrounds. As we showed in Section 5.6, a sample of collision events can be described by a double Gaussian timing distribution. Said differently, all the collision backgrounds are well described by six parameters, namely the mean and RMS of the two Gaussians (the right and wrong vertex) as well as their normalizations.

While the mean of the wrong vertex may vary sample to sample, as we have seen in Section 5.6, three out of six of these parameters do not change from sample to sample and all that is left is to determine the wrong vertex mean and the relative normalization in order to have a full understanding of the collision backgrounds. With this in hand we can make a prediction of the number of events in the signal region.

In Chapter 3 we laid out this argument, with the conclusion summarized in Equation 3.11, that it is straightforward to predict the number of events in the signal region (N_{SR}) if you know $\langle t_{corr}^{WV} \rangle$ distribution and the number of events in the control region (N_{CR}). This result is visualized in Figure 3.2 with the double Gaussian assumption for various wrong vertex means where we ignore the contribution from the right vertex sample and cosmoics. This assumption is typically true for wrong vertex fractions of $\sim 10\%$ or greater. The yellow band represents a systematic uncertainty in the RMS of the wrong vertex of ± 0.1 ns which is the one of the systematic uncertainties we will take into account when predicting the expected number of events in the signal region from SM sources. It should be noted here that we are only trying to predict the number of background events from SM contributions in the signal region. At no point have we used any information about the number of

events in the signal region nor anything about the shape of the timing distribution in the signal region except that SM sources will be Gaussian.

We now test the hypothesis put forward in Equation 3.11 by looking at how well the prediction between the wrong vertex mean and the ratio of events in the signal and control regions holds in our various MC and data control samples. Figure 6.1 shows the results of the counting experiment for the various MC and $e+\cancel{E}_T$ data control samples that pass all the selection requirements in Table 5.5 for photons and Table 5.2 for electrons. In this case we count the number of events in the signal and control regions and compute the ratio; note that the error is just the statistical error on the sample. We then plot this versus the fitted wrong vertex mean when we fit the various samples in the region $-10 \text{ ns} < t_{corr} < 10 \text{ ns}$ using the double Gaussian assumption where the mean and RMS of the right vertex are fixed to 0.0 ns and 0.65 ns respectively and the RMS of the wrong vertex is fixed to 2.0 ns as shown in Figure 5.14. The results of these fits are summarized in Table 6.1.

Sample	Observed Wrong Vertex Mean (ns)	Predicted Ratio	Observed Ratio
$W \rightarrow e\nu$ MC	$0.73 \pm 0.19 \text{ ns}$	2.92 ± 1.01	3.70 ± 0.36
$\gamma + \text{Jet}$ MC	$0.18 \pm 0.13 \text{ ns}$	1.30 ± 0.26	1.30 ± 0.20
$W\gamma$ MC	$0.14 \pm 0.07 \text{ ns}$	1.22 ± 0.14	1.14 ± 0.11
$Z\gamma$ MC	$0.12 \pm 0.01 \text{ ns}$	1.20 ± 0.01	1.12 ± 0.02
$W \rightarrow \mu\nu$ MC	$0.29 \pm 0.26 \text{ ns}$	1.50 ± 0.70	1.40 ± 0.41
$W \rightarrow \tau\nu$ MC	$0.43 \pm 0.26 \text{ ns}$	1.90 ± 0.90	1.70 ± 0.40
$e + \cancel{E}_T$ Data	$0.16 \pm 0.05 \text{ ns}$	1.26 ± 0.16	1.32 ± 0.17
$e + \cancel{E}_T$ Data ($E_T > 30 \text{ GeV}$ and $\cancel{E}_T > 30 \text{ GeV}$)	$0.04 \pm 0.05 \text{ ns}$	1.03 ± 0.07	1.06 ± 0.13

Table 6.1

Summary of the results shown in Figure 6.1 showing the predicted and observed ratio of the number of events in the signal region ($2 \text{ ns} < t_{corr} < 7 \text{ ns}$) to the number of events in the control region ($-7 \text{ ns} < t_{corr} < -2 \text{ ns}$) for our six MC and two $e + \cancel{E}_T$ control samples. The observed wrong vertex mean here is measured using a double Gaussian fit to the data and assuming a right vertex mean = 0.0 ns and RMS = 0.65 ns as well as a wrong vertex RMS=2.0.

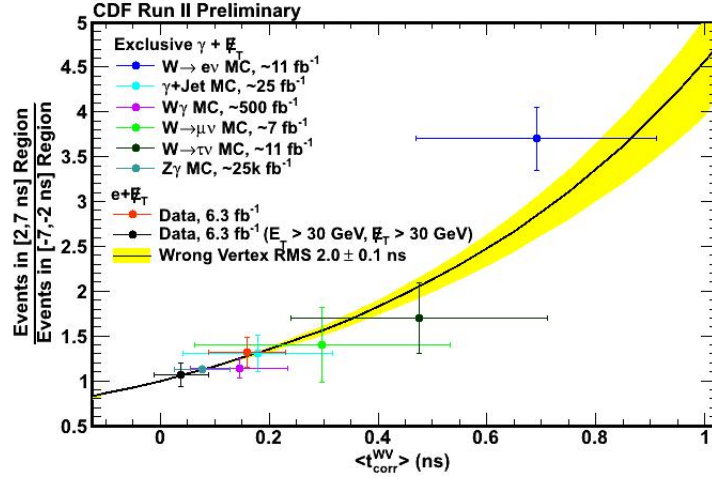


Fig. 6.1. Ratio of the number of events observed in the signal region ($2 \text{ ns} < t_{\text{corr}} < 7 \text{ ns}$) to the number of event observed in the control region ($-7 \text{ ns} < t_{\text{corr}} < 2 \text{ ns}$) versus the measured wrong vertex mean for our eight control samples. The black line is not a fit, but rather is the prediction from the double Gaussian assumption where the right vertex distribution is fixed and the wrong vertex mean is allowed to vary. It does an excellent job of predicting the numer of events in the signal region. Note that in this figure we have measured $\langle t_{\text{corr}}^{\text{WV}} \rangle$ from a full fit of the control sample (see Figure 5.14), which we cannot do directly in the real data.

The various sample points clearly follow the expected relationship and demonstrate that our distributions are well modeled by our double Gaussian assumption. Note that the line in Figure 6.1 is not a fit, but is simply the prediction from Equation 3.11. This remarkable result means that for a sample of collision events in the exclusive $\gamma + \cancel{E}_T$ final state, that once we are able to determine the wrong vertex mean and we count the number of events in the control region from collision sources we can determine the number of events expected in the signal region. The task of finding an independent way of determining the wrong vertex mean, and thus measuring the bias present in the sample, is the subject of the next section. We note that additional studies show that this is true, to within the stated uncertainties even

if the sample is made of two very different vertex means because the means are small compared to the overall 2.0 ns RMS [75].

6.2 Measuring the Wrong Vertex Mean for the Sample

The first thing that is important to note, as we now turn our attention to establishing a way to measure the wrong vertex mean, is that naively we may attempt to establish the mean of the wrong vertex by simply fitting the full data sample from $-7 \text{ ns} < t_{corr} < +2 \text{ ns}$ and then extrapolating this fit into the signal region. While this should work in the limit of having infinite statistics, this method does not work in our data for three major reasons:

- 1) Events from cosmic rays constitute a significant fraction of the number of events in the region from $-7 \text{ ns} < t_{corr} < -2 \text{ ns}$ and thus may distort the wrong vertex distribution in this area.
- 2) In the region from $-2 \text{ ns} < t_{corr} < 2 \text{ ns}$ events from the right vertex dominate thus making it difficult to measure the mean of the wrong vertex in this region.
- 3) All of these problems are compounded as the wrong vertex mean becomes larger. Said differently, as the wrong vertex mean gets larger the distribution in the control region ($-7 \text{ ns} < t_{corr} < -2 \text{ ns}$) only gives a smaller and smaller fraction of the events from which to estimate the mean.

With these problems in mind, we consider an orthogonal set of events that allows us to measure $\langle t_{corr}^{WV} \rangle$. For such a sample we look to the events that pass all of our exclusive $\gamma + \cancel{E}_T$ requirements (outlined in Table 5.5) but do not have a reconstructed SpaceTime vertex. As illustrated in Figure 6.2, we refer to this sample as the “no vertex” sample. We expect this sample to be very similar to the wrong vertex events for a number of reasons. The first is that in wrong vertex events they may or may not have had their true vertex reconstructed. We note that in our MC backgrounds

samples where we selected the wrong vertex, the right vertex was only available to be selected a small fraction ($\sim 50\%$) of the time. Furthermore, we expect the topology of the events where we select a wrong vertex to be similar to those with no vertex. We will check this assumption in more detail after we describe more about the timing we use for no vertex events.

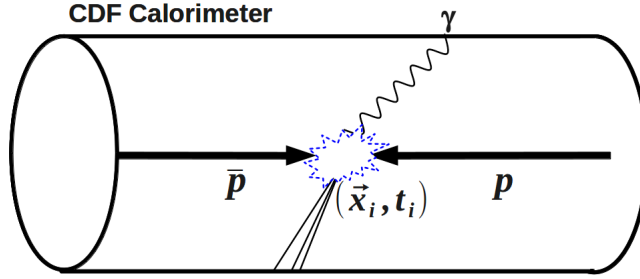


Fig. 6.2. This figure shows the creation of a $\gamma + \cancel{E}_T$ event where the primary collision does not produce a reconstructed vertex. We use a sample of events with this topology because their timing distribution, t_{corr}^0 , is dominated by the topology of the SM events where the wrong vertex is selected. If no good SpaceTime vertex is reconstructed, but the event passes all the other exclusive $\gamma + \cancel{E}_T$ event selection requirements there is a clear relationship between $\langle t_{corr}^0 \rangle$ and $\langle t_{corr}^{WV} \rangle$.

If no good SpaceTime vertex is reconstructed, but the event passes all the other exclusive $\gamma + \cancel{E}_T$ event selection requirements we can still construct t_{corr}^0 where we assume the initial time and position was $t_0 = 0$ ns and $z = 0$ cm respectively. This is a reasonable assumption on average since this is the most common place for collisions to occur. From this point, we can see why moving to E_T^0 and \cancel{E}_T^0 , as was described in Section 5.5.1, was doubly advantageous. In addition to reducing the bias in the t_{corr}^{WV} distribution, we can select this sample in exactly the same way as the main sample regardless of whether there is a vertex reconstructed in the event.

While we expect this sample to be dominated by cosmic ray backgrounds, the events from a collision which had no reconstructed vertex should have the same underlying physics and topology and thus the same timing bias as the wrong vertex distribution. We can see this by rewriting Equation 1.8 for t_{corr}^0

$$t_{corr}^0 = t_f - t_0 - \frac{|\vec{x}_f - \vec{x}_0|}{c} \quad (6.1)$$

where t_0 and x_0 are measured at the center of the detector. However, as we saw in Equation 5.2, we can rewrite t_f as

$$t_f = t_{RV} + TOF_{RV} \quad (6.2)$$

Plugging this in and setting $\frac{\vec{x}_f - \vec{x}_0}{c} = TOF_0$ and $t_0 = 0$ ns we find

$$t_{corr}^0 = TOF_{RV} + t_{RV} - TOF_0 \quad (6.3)$$

where TOF_0 is the predicted time of flight from $z=0$ cm to the calorimeter position. Since many of these terms are the same as in the t_{corr}^{WV} equation described in Equation 5.3 we can plug this relation in to find

$$t_{corr}^{WV} = t_{corr}^0 - t_{WV}^0 + (TOF_0 - TOF_{WV}). \quad (6.4)$$

This relationship is useful because what we are after is $\langle t_{corr}^{WV} \rangle$. Since the three terms in Equation 6.4 are not correlated with one another, or are small, we can consider each term independently in terms of its contribution to $\langle t_{corr}^{WV} \rangle$. We can directly measure $\langle t_{corr}^0 \rangle$ distribution from the data. The t_{WV}^0 distribution is zero purely from beam related parameters with a mean of 0 ns and an RMS of 1.28 ns as shown in Figure 3.10. Finally, we note that $TOF_0 - TOF_{WV}$ term is fairly narrow and has a mean of ~ 0 ns for geometric reasons. This is true because wrong vertices are produced independently of the physics of the right vertex, so

$TOF_0 - TOF_{WV}$ is largely process independent. A representation of this can be seen on the LHS of Figure 6.3. We note that the distance from the beam line to the calorimeter is much larger (~ 184 cm) than the scale of the variation in the collision distribution (RMS of ~ 28 cm shown in Section 2.4.5). This fact implies that $TOF_0 - TOF_{WV}$ should be small on average. The RHS of Figure 6.3 shows this quantitatively in a series of toy pseudo-experiments where we calculate the time-of-flight of the wrong vertex, TOF_{WV} , and the time-of-flight for the no vertex, TOF_0 , distributions. Here we generate vertices according to the z and t parameters of the Tevatron beam in Table 2.1 and assume a uniform arrival in the CES z position. We see that $\langle TOF_0 - TOF_{WV} \rangle$ is consistent with zero to less than 40 ps. With this understanding we see why, to a good degree of approximation, $\langle t_{corr}^{WV} \rangle = \langle t_{corr}^0 \rangle$.

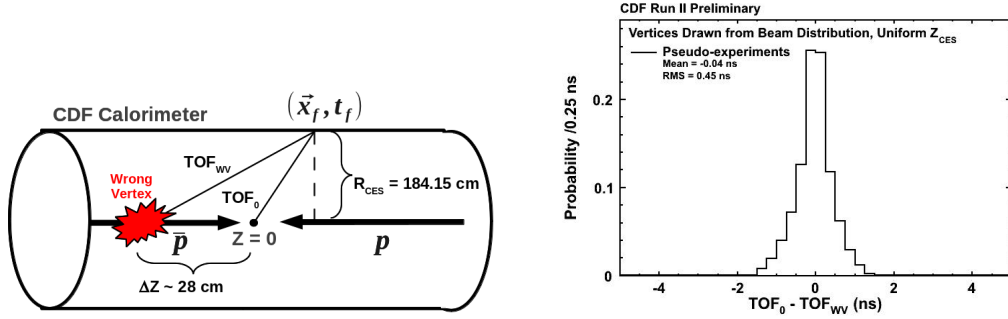


Fig. 6.3. (LHS) An illustration showing the various components of the time-of-flight components of the t_{corr}^{WV} coming from the difference relative to the center of the detector (TOF_0) and the time-of-flight difference relative to a wrong vertex (TOF_{WV}). (RHS) The results of toy pseudo-experiments where vertices are generated according to the z and t parameters of the Tevatron and we calculate the time-of-flight of the wrong vertex, TOF_{WV} , and the time-of-flight for the no vertex, TOF_0 demonstrating that $\langle TOF_0 - TOF_{WV} \rangle = 0$ to less than 40 ps.

To test this hypothesis we use our six MC control samples as well as our two $e + \cancel{E}_T$ data control samples. We select events using Tables 5.5 for photons and 5.2 for electrons but this time require these samples to explicitly fail the good SpaceTime

vertex selection in order to construct the no vertex timing distribution. We examine t_{corr}^0 for each sample, shown in Figure 6.4, and fit a Gaussian from $-5 \text{ ns} < t_{corr}^0 < 3 \text{ ns}$ allowing the mean to vary and find the best fit parameter while fixing the RMS= 1.6 ns. We pick the range for the Gaussian fit to start at -5 ns in order to avoid any potential contamination from beam halo events which we expect to begin to be present at $t_{corr}^0 < -5 \text{ ns}$, as described in Section 4.3. We only fit out to $t_{corr}^0 = 3 \text{ ns}$ in order to avoid any potential contamination from signal like events that we expect to see above 3 ns, as described in Section 1.5. We choose the RMS= 1.6 ns since this is the expected t_{corr}^0 timing resolution as described in Section 5.1. We also note that for the control $e + \bar{E}_T$ samples from data we include a fit to the cosmics by extrapolating to the cosmics region $20 \text{ ns} < t_{corr} < 80 \text{ ns}$. The results for all eight are shown in Figure 6.4.

To test the assumption that the t_{corr}^0 distribution is well modeled by a Gaussian with an RMS= 1.6 ns we do a second fit with a Gaussian in the range $-5 \text{ ns} < t_{corr}^0 < 3 \text{ ns}$ and allow both the mean and RMS to vary and find the best fit parameter for each sample. The results are summarized Table 6.2 and can be seen graphically in Figure 6.5. We find that, as expected, the mean varies but is again independent of RMS. Similarly, we note that the data points all fall within the yellow band ($\pm 10\%$ the nominal RMS) for a wide range of $< t_{corr}^0 >$.

Having established the assumption that the no vertex timing distribution is accurately described by a Gaussian with an RMS of 1.6 ns for our MC backgrounds and $e + \bar{E}_T$ data, we now look to the comparison of $< t_{corr}^{WV} >$ (which we can measure for our control samples since we know the true vertex, but not the real data) versus $< t_{corr}^0 >$ (which we can measure with real data). In Figure 6.6, and summarized in Table 6.3, we compare the two measured timing means. We quickly notice that all of the points lie on the line at 45 degrees (where the two measured timing means equal one another). The mean of the wrong vertex and the mean of the no vertex

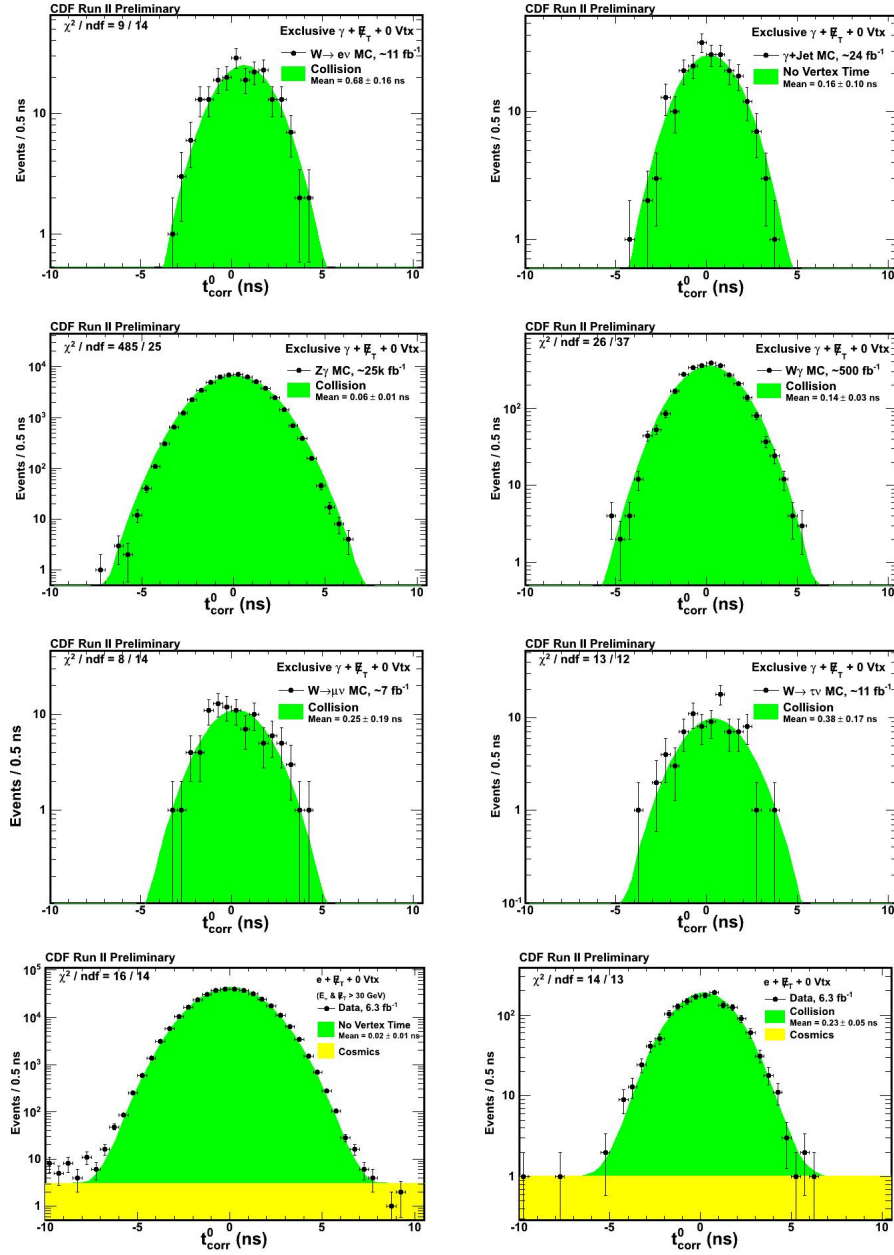


Fig. 6.4. The t_{corr}^0 distribution for the no vertex samples from the six MC control samples as well as the two control e^+e^- sample from data. The fit is for a Gaussian fit from $-5 \text{ ns} < t_{corr}^0 < 3 \text{ ns}$ with a fixed $\text{RMS} = 1.6 \text{ ns}$ in order to estimate to measure $\langle t_{corr}^0 \rangle$ which is a good estimate of $\langle t_{corr}^{WV} \rangle$.

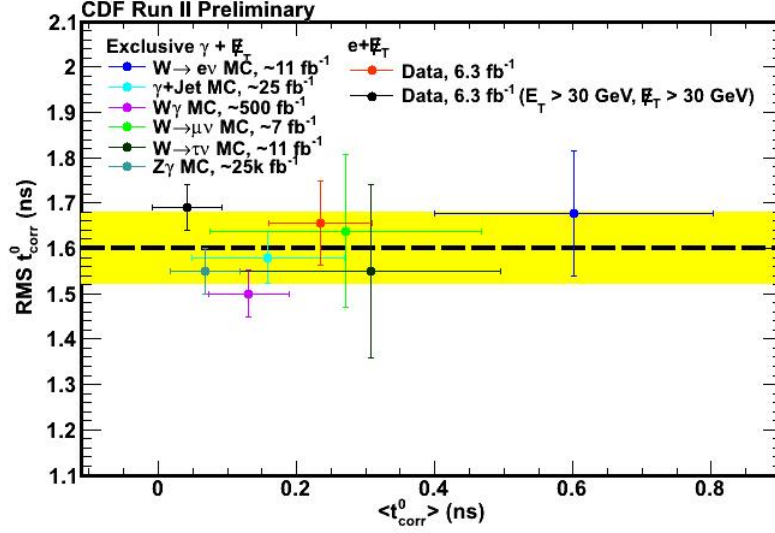


Fig. 6.5. A plot showing the relationship between the RMS of the t_{corr}^0 distribution for no vertex events versus $\langle t_{corr}^0 \rangle$ for our MC and $e+\cancel{E}_T$ data control samples. This demonstrates that the assumption that the no vertex corrected time distribution is well modeled by a Gaussian with an $\text{RMS} = 1.6 \pm 0.08$ ns for the various MC backgrounds in addition to $e+\cancel{E}_T$ data samples is a good one. The no vertex mean and RMS is found by fitting the no vertex corrected time (t_{corr}^0) distribution with a single Gaussian from $-5 \text{ ns} < t_{corr}^0 < 3 \text{ ns}$ where the Gaussian RMS and mean are allowed to vary to find the best fit.

distribution are thus shown to be nearly equivalent values for our six MC control samples as the two control $e+\cancel{E}_T$ data samples.

We note that although the two are always equal within uncertainties, the two measurements are not always identical, so for this reason we conservatively overestimate any systematic difference between the wrong vertex mean and the no vertex mean to be 100 picoseconds.

Sample	No Vertex Mean (ns)	No Vertex RMS (ns)
$W \rightarrow e\nu$ MC	0.61 ± 0.20 ns	1.68 ± 0.14 ns
$\gamma + \text{Jet}$ MC	0.16 ± 0.11 ns	1.58 ± 0.06 ns
$Z\gamma$ MC	0.07 ± 0.05 ns	1.55 ± 0.05 ns
$W \rightarrow \mu\nu$ MC	0.27 ± 0.20 ns	1.64 ± 0.17 ns
$W \rightarrow \tau\nu$ MC	0.31 ± 0.19 ns	1.56 ± 0.19 ns
$W\gamma$ MC	0.13 ± 0.06 ns	1.50 ± 0.05 ns
$e + \cancel{E}_T$ Data	0.23 ± 0.08 ns	1.66 ± 0.09 ns
$e + \cancel{E}_T$ Data ($E_T \& \cancel{E}_T > 30$ GeV)	0.04 ± 0.05 ns	1.69 ± 0.05 ns

Table 6.2

Summary of the results in Figure 6.5 which plots the relationship between the mean and RMS of the t_{corr}^0 distributions for the six MC and two $e + \cancel{E}_T$ control datasets for sets of events where we require the events to pass all the requirements in Tables 5.5 and 5.2 but have no SpaceTime vertex reconstructed. The $\langle t_{corr}^0 \rangle$ and RMS is found by fitting the no vertex corrected time (t_{corr}^0) distribution with a single Gaussian from $-5 \text{ ns} < t_{corr}^0 < 3 \text{ ns}$ where the Gaussian RMS and mean are allowed to vary to find the best fit.

With this assumption, we can rewrite Equation 3.11 using $\mu^{NV} = \langle t_{corr}^0 \rangle$ and $\mu^{WV} = \langle t_{corr}^{WV} \rangle$ and determine the number of events in the signal region from collision backgrounds using the relation:

$$N_{signal}^{SM} = R(\mu^{WV} = \mu^{NV}) \cdot N_{control}^{SM} \quad (6.5)$$

and take the systematics on R due to the uncertainty between the relation $\mu^{WV} = \mu^{NV}$ and the uncertainty of the RMS of the wrong vertex Gaussian.

To test how well this relation predicts the number of events in the signal region with our eight control samples we show the results in Figure 6.7 as if they were real data. By comparing the prediction we see that the measured value of $\langle t_{corr}^0 \rangle$ does an excellent job of predicting the ratio of events in the sample of events with

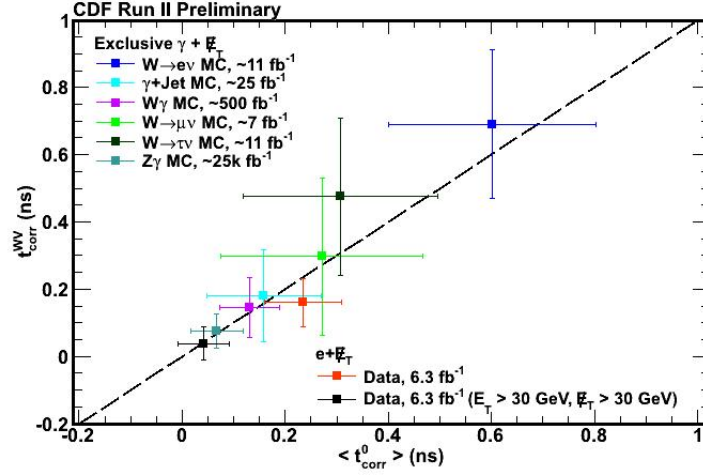


Fig. 6.6. The correlation between $\langle t_{corr}^{WV} \rangle$ and $\langle t_{corr}^0 \rangle$ for our MC and $e + \cancel{E}_T$ data control samples. One method is taken from Table 5.6 and is where we measure the WV directly from a full fit to the data, which is only possible in MC, and one from the no-vertex sample which is available in data. Note that the two agree to a high degree of precision. This fact allows us to predict the wrong vertex mean for a given sample by measuring a sample of events that pass all the other selection requirements but fail to reconstruct a vertex.

a good vertex. Again, the black line is a prediction based on the measure $\langle t_{corr}^0 \rangle$ and not a fit. A comparison of the the measured and observed ratio is given in Table 6.4. Thus, we have confirmed that our method that uses an independent sample, the “no vertex” sample, in conjunction with the number of events in the control region gives us a data-driven estimate of the number of events in the signal region for SM backgrounds. The uncertainty, as we will see is dominated by the statistical uncertainty of the number of events from collision in the no vertex sample to determine $\langle t_{corr}^0 \rangle$.

In the next section we formalize the background estimation procedure in the exclusive $\gamma_{delayed} + \cancel{E}_T$ final state utilizing the fact that we can predict the wrong

Sample	Wrong Vertex Mean (ns)	No Vertex Mean (ns)
$W \rightarrow e\nu$ MC	0.73 ± 0.19 ns	0.68 ± 0.16
γ +Jet MC	0.18 ± 0.13 ns	0.16 ± 0.10
$W\gamma$ MC	0.14 ± 0.07 ns	0.14 ± 0.03
$Z\gamma$ MC	0.12 ± 0.01 ns	0.06 ± 0.01
$W \rightarrow \mu\nu$ MC	0.29 ± 0.26 ns	0.25 ± 0.19
$W \rightarrow \tau\nu$ MC	0.43 ± 0.26 ns	0.38 ± 0.17
$e + \cancel{E}_T$ Data	0.16 ± 0.05 ns	0.23 ± 0.05
$e + \cancel{E}_T$ Data ($E_T > 30$ GeV and $\cancel{E}_T > 30$ GeV)	0.04 ± 0.05 ns	0.02 ± 0.01

Table 6.3

Summary of the two different measurements of the wrong vertex mean using the six MC backgrounds control samples, selected using Table 5.5, and the two $e + \cancel{E}_T$ data control samples, selected using Table 5.2. Here we obtain the wrong vertex mean by fitting the corrected time (t_{corr}) distribution with a double Gaussian function from $-10 \text{ ns} < t_{corr} < 10 \text{ ns}$ where the right vertex Gaussian mean = 0.0 ns and RMS = 0.65 ns and the wrong vertex Gaussian RMS = 2.0 ns and the mean is allowed to vary to find the best fit. The no vertex mean is found by fitting the no vertex corrected time (t_{corr}^0) distribution with a single Gaussian from $-5 \text{ ns} < t_{corr}^0 < 3 \text{ ns}$ where the Gaussian RMS = 1.6 ns and the mean is allowed to vary to find the best fit. These results are plotted in Figure 6.6.

vertex mean from the “no vertex” sample, but at the same time take into account the contributions from cosmic ray background sources.

6.3 The Combined Background Estimation Procedure

To briefly recap, in Section 6.1 we demonstrated how the double Gaussian nature of the corrected time distribution makes it possible to predict the number of events expected in the signal region ($2 \text{ ns} < t_{corr} < 7 \text{ ns}$) from SM sources if we know the mean of the wrong vertex distribution. In Section 6.2 we showed how we can estimate the wrong vertex mean using a sample of events that pass all our event

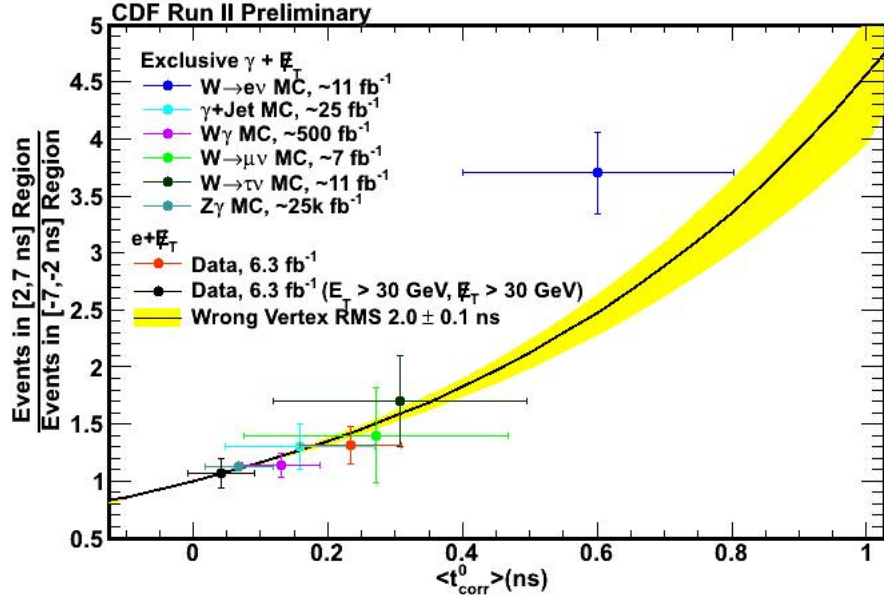


Fig. 6.7. The ratio of the number of events observed in the signal region ($2 \text{ ns} < t_{\text{corr}} < 7 \text{ ns}$) to the number of event observed in the control region ($-7 \text{ ns} < t_{\text{corr}} < -2 \text{ ns}$) versus the observed “no vertex” mean for the eight MC and data control samples. This shows that using the double Gaussian assumption and measuring the mean of the “no vertex” distribution we can accurately predict the number of events in the signal region for all our control samples within uncertainties.

selection requirements but fail to reconstruct a vertex and measure $\langle t_{\text{corr}}^0 \rangle$. In Section 4.2 we outlined how we estimate the cosmic ray rate in the signal region by measuring the number of events in the cosmics region ($20 \text{ ns} < t_{\text{corr}} < 80 \text{ ns}$) where we do not expect to see any collision sources which we call this the “cosmics region”.

We now combine these two estimate and lay out the final procedure by which we will use the information from the cosmics region, the mean of the no vertex distribution, and the number of events observed in the control region ($-7 \text{ ns} < t_{\text{corr}} < -2 \text{ ns}$) to predict the number of events expected in the signal region ($2 \text{ ns} < t_{\text{corr}} < 7 \text{ ns}$) from SM sources. We procedure is as follows:

Sample	Observed No Vertex Mean (ns)	Predicted Ratio	Observed Ratio
W→ eν MC	0.68 ± 0.16 ns	2.74 ± 0.76	3.70 ± 0.36
γ+Jet MC	0.16 ± 0.10 ns	1.27 ± 0.20	1.30 ± 0.20
Wγ MC	0.14 ± 0.03 ns	1.23 ± 0.05	1.14 ± 0.11
Zγ MC	0.06 ± 0.01 ns	1.09 ± 0.02	1.12 ± 0.02
W→ μν MC	0.25 ± 0.19 ns	1.46 ± 0.48	1.40 ± 0.41
W→ τν MC	0.38 ± 0.17 ns	1.77 ± 0.51	1.70 ± 0.40
e+ \cancel{E}_T Data	0.23 ± 0.05 ns	1.39 ± 0.31	1.32 ± 0.17
e+ \cancel{E}_T Data ($E_T > 30$ GeV and $\cancel{E}_T > 30$ GeV)	0.02 ± 0.01 ns	1.03 ± 0.07	1.06 ± 0.13

Table 6.4

Summary of the results shown in Figure 6.7 of our method for the SM MC samples and our $e + \cancel{E}_T$ “no vertex” control samples. We find the predicted ratio using that measured mean as well as the observed ratio of the number of events in the signal region to the control region agree to within errors.

- **Select events for the exclusive $\gamma + \cancel{E}_T$ final state:**

All events are selected using the criteria in Table 5.5. We sort events into events that have a good SpaceTime vertex and events with no good SpaceTime vertex. From this bifurcation we construct the corrected time distributions for each. For the events having a good SpaceTime vertex we construct the t_{corr} variable defined in Equation 1.8. Events that do not have a good SpaceTime vertex are part of the “no vertex” sample and we construct the t_{corr}^0 timing distribution defined in Equation 6.4.

- **Estimate the cosmic ray event rate:**

Since events from cosmic rays represent a significant contribution for both the good vertex and no vertex sample, we must estimate their contamination to the regions under consideration. Thus, for both the t_{corr} and t_{corr}^0 timing distributions, we look at the events in the timing region from $20 \text{ ns} < t_{corr} < 80 \text{ ns}$ and $20 \text{ ns} < t_{corr}^0 < 80 \text{ ns}$ and fit a straight line in this region. This fitted

rate gives us an estimate of the rate of cosmics per nanosecond present in both the no vertex and good vertex samples (which is expected to be different for each). This is then straightforwardly extrapolated to the number of events in the signal region using Equation 4.3 and a similar relation for the no vertex sample.

- **Measure the mean of the “no vertex” timing distribution:**

Using the t_{corr}^0 distribution, we fit a straight line fixed at the cosmics rate plus a Gaussian with an RMS = 1.6 ns from $-5 \text{ ns} < t_{corr}^0 < 3 \text{ ns}$ and measure the mean of this distribution and the uncertainty of the fit.

- **Predict the number of background events in the Signal Region:**

Finally, using the mean of the no vertex distribution, the measured cosmics rate for the good vertex sample, and the number of events observed in the control regions in the good vertex sample we can uniquely calculate the number of events expected from SM sources using Equation 6.5. With this prediction we can sum the number of events from both cosmics and wrong vertex events in the signal region as well as determine the uncertainty on this estimation.

With the data-driven background procedure now laid out, we now turn to the results of the search in the exclusive $\gamma + \cancel{E}_T$ final state and the quantification of the associated errors with our prediction. Ultimately, the difference between the predicted number of events in the signal region and the observed number will indicate whether we have evidence for new physics in the exclusive $\gamma_{delayed} + \cancel{E}_T$ final state.